# Multistep, Low-Temperature Pseudomorphic Transformations of Nanostructured Silica to Titania via a Titanium Oxyfluoride Intermediate

Justin C. Lytle, Hongwei Yan, Ryan T. Turgeon, and Andreas Stein*

*Department of Chemistry, University of Minnesota, 207 Pleasant Street SE, Minneapolis, Minnesota 55455*

*Received March 25, 2004. Revised Manuscript Received July 8, 2004*

Synthetic silica preforms with an inverse opal or three-dimensionally ordered macroporous (3DOM) structure were converted to 3DOM $TiOF_2$ and subsequently to 3DOM $TiO_2$ by solid−gas pseudomorphic transformation reactions, reactions which maintain the shape and structural features of the original material. 3DOM $SiO_2$ preforms with periodic arrays of macropores and hierarchical feature sizes (e.g., macropore separation 334 nm, average wall thickness 59 nm) were prepared by colloidal crystal templating. They were reacted with $TiF_4$ in sealed steel pipes at 190, 235, and 300 °C. At 190 °C no conversion took place, while at 300 °C the material was converted mostly to crystalline $TiOF_2$ with an irregular structure. However, at 235 °C the periodic macroporous structure of the preform was maintained with little change in average pore separation. In these samples, the initially smooth wall structure of 3DOM $SiO_2$ was largely replaced by interconnected $TiOF_2$ cubes with edge lengths of 133 nm. The X-ray diffraction (XRD) pattern showed sharp lines of $TiOF_2$. The product exhibited opalescence similar to that of the preform, giving a visual confirmation of the success of the pseudomorphic transformation on an extended length scale. An analogous transformation was also investigated with spherical silica preforms. Different stages of transformation were observed by scanning electron microscopy, permitting a discussion of critical parameters in these conversions. The macroporous $TiOF_2$ product was subsequently converted to $TiO_2$ (anatase) by reaction with moist air at 300 °C. In this reaction, pseudomorphism was observed on the scale of tens of micrometers, on the submicrometer macropore scale, and on the scale of the cubic particles forming the wall skeleton. The sample was still composed of interconnected cubes with similar edge lengths, and the pore spacing was nearly maintained. XRD showed only $TiO_2$ anatase reflections. The synthetic paradigms demonstrated for the silica to anatase conversion may be transferable to other 2D or 3D material shapes within the applicable range of feature sizes.

## Introduction

In the past decade, a large palette of techniques has been developed to chemically synthesize materials with structural features ranging over wide length scales. While such architectural control has been applied to many compositions, the structural variety of silica on all length scales is rivaled by few, if any, other inorganic compositions.[1−3] In particular on the micrometer and nanometer scales, the ability to structure other ceramic or metallic compositions with the complex architectures found in silica would benefit many materials and device applications. A possible approach to transcribe shapes is by pseudomorphic transformations, reactions in which preforms are converted to other compositions while the shape and structural features of the original material are maintained. Several examples of pseudomorphic experiments have been reported based on preforms including bioclastic siliceous materials,[4,5] synthetic silica[6] and alumina gels,[7] minerals,[8,9] salts,[10] and ceramics[11−22] to prepare metal oxides, nitrides, carbides, metals, and ceramic/metal composites.

Except for recent work involving diatoms, these pseudomorphic transformations have been applied mostly

* To whom correspondence should be addressed. Phone: (612) 624-1802. Fax: (612) 626-7541. E-mail: stein@chem.umn.edu.

(1) Iler, R. K. *The Chemistry of Silica*; Wiley: New York, 1979.
(2) Brinker, C. J.; Scherer, G. W. *Sol−Gel Science: The Physics and Chemistry of Sol−Gel Processing*; Academic Press: San Diego, CA, 1990.
(3) Wright, J. D.; Sommerdijk, N. A. J. M. *Sol−Gel Materials Chemistry and Applications*; Gordon and Breach Science Publishers: Amsterdam, 2001.
(4) Harker, R. I. *Science* **1971**, *173*, 235−237.
(5) Sandhage, K. H.; Dickerson, M. B.; Huseman, P. M.; Caranna, M. A.; Clifton, J. D.; Bull, T. A.; Heibel, T. J.; Overton, W. R.; Schoenwaelder, M. E. A. *Adv. Mater.* **2002**, *14*, 429−433.
(6) Martin, T.; Galarneau, A.; Di Renzo, F.; Fajula, F.; Plee, D. *Angew. Chem., Int. Ed.* **2002**, *41*, 2590−2592.
(7) Sanchez-Valente, J.; Bokhimi, X.; Hernandez, F. *Langmuir* **2003**, *19*, 3583−3588.
(8) Golden, D. C.; Chen, C. C.; Dixon, J. B.; Tokashiki, Y. *Geoderma* **1988**, *42*, 199−211.
(9) Sipple, E.; Bracconi, P.; Dufour, P.; Mutin, J. *Solid State Ionics* **2001**, *141−142*, 455−461.
(10) Bamberger, C. E. *J. Mater. Sci. Lett.* **1996**, *15*, 162−165.
(11) Lee, J. S.; Volpe, L.; Ribeiro, F. H.; Boudart, M. *J. Catal.* **1988**, *112*, 44−53.
(12) Bamberger, C. E.; Alexander, K. B. *J. Cryst. Growth* **1993**, *126*, 525−529.
(13) Bamberger, C. E. *J. Mater. Sci. Lett.* **1994**, *13*, 1742−1745.
(14) Tan, B. J.; Xiao, Y.; Galasso, F. S.; Suib, S. *Chem. Mater.* **1994**, *6*, 918−926.

10.1021/cm049489b CCC: $27.50 
Published on Web 08/25/2004

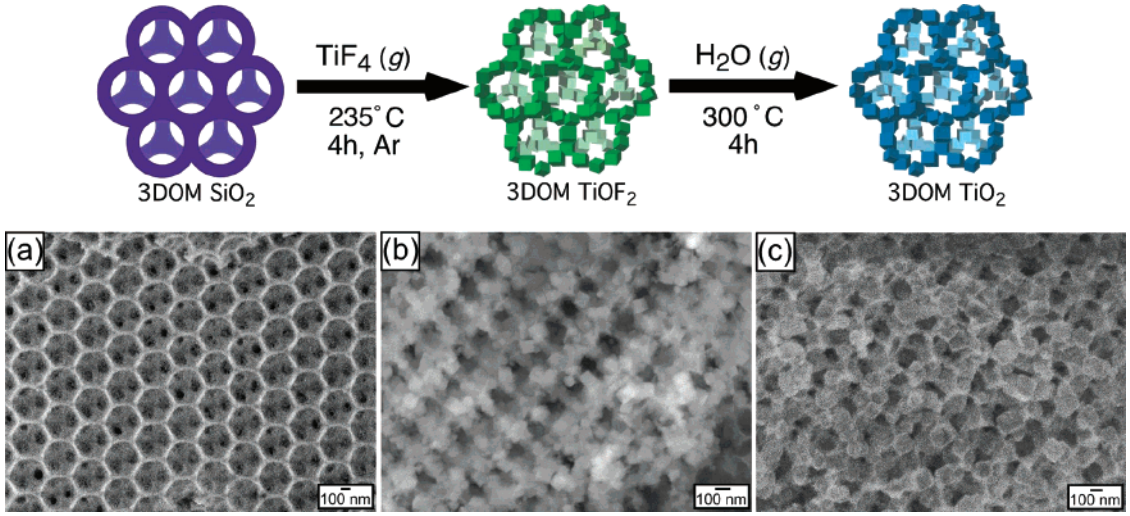


**Figure 1.** Schematic overview of conversion steps needed to transform (a) 3DOM $SiO_2$ into (b) 3DOM $TiOF_2$ via $TiF_4$ vapor generated at 235 °C and then into (c) 3DOM $TiO_2$ by heating at 300 °C in moist air. These images correspond to data series 1 in Table 1. All subsequent images except for Figure 5a correspond to data series 2.

to micrometer-sized or larger bulk objects. To evaluate the applicability of pseudomorphic transformations to nanostructures, a synthetic silica preform with hierarchical feature sizes was chosen in this study: the inverse opal or three-dimensionally ordered macroporous (3DOM) structure. 3DOM $SiO_2$ prepared by colloidal crystal templating consists of smooth amorphous silica walls (typically tens of nanometers in thickness) that encompass three-dimensionally interconnected spherical voids hundreds of nanometers in diameter (Figure 1a). This structure can be prepared as thin films, small particles, and monoliths.[23−27] These materials have relatively large specific surface areas and appear opalescent due to the diffraction of visible light by the periodic structure. The periodic arrangement of macropores permits easy comparison of the structure before and after conversion. For further comparison, spherical $SiO_2$ preforms were also examined.

In this study, multistep gas−solid reactions at relatively low temperatures were employed to pseudomorphically convert the amorphous 3DOM $SiO_2$ skeleton to nanocrystalline $TiOF_2$ and then to $TiO_2$ (Figure 1). Initially, the direct conversion of 3DOM $SiO_2$ into 3DOM $TiO_2$ using $TiF_4$ vapor (eq 1) was considered, on the

$$TiF_4(g) + SiO_2(s) \rightarrow TiO_2(s) + SiF_4(g) \qquad (1)$$

basis of its thermodynamic feasibility at relatively low temperatures and because of the interest in $TiO_2$ due to its photocatalytic and oxygen-sensing properties, its relatively high refractive index, and its potential benefits in photonic crystal structures. $\Delta G_f$ for this reaction is −88 kJ/mol at 127 °C and remains negative at temperatures exceeding 1000 °C.[28] Previously published thermodynamic calculations suggested that this reaction should proceed sufficiently at 900 °C.[5] Given the relatively high vapor pressure of $TiF_4$ (ca. 100 Torr at 235 °C), much lower reaction temperatures were chosen here to minimize grain growth and sintering and to maintain the nanostructure of the preform. At these low temperatures, crystalline $TiOF_2$ nanocubes that partially replicated the 3DOM structure were formed, with only minor amounts of the anticipated $TiO_2$ product detected by electron microprobe analysis (eq 2). A second conversion of the ordered macroporous product composed of $TiOF_2$ cubic crystallites with water vapor further altered the sample's composition to anatase $TiO_2$, completing the indirect transformation of 3DOM $SiO_2$ into 3DOM $TiO_2$. In all reactions the periodic macroporous structure of the preform was maintained within a limited temperature window. In the second transformation step, pseudomorphism was also observed in the cubic shape of the nanocrystals forming the inverse opal skeleton.

$$2TiF_4(g) + SiO_2(s) \rightarrow 2TiOF_2(s) + SiF_4(g) \qquad (2)$$

## Experimental Section

**Materials.** Reagents were obtained from the following sources: absolute ethanol was from Aaper Alcohol and Chemical Co.; methyl methacrylate monomer (MMA; 99%), 2,2′-azobis(2-methylpropionamidine) dihydrochloride initiator (97%),

(15) Breslin, M. C.; Ringnalda, J.; Xu, L.; Fuller, M.; Seeger, J.; Daehn, G. S.; Otani, T.; Fraser, H. L. *Mater. Sci. Eng., A* **1995**, *195*, 113−119.
(16) Torardi, C. C.; Horowitz, H. S. *J. Solid State Chem.* **1995**, *119*, 349−358.
(17) Ewsuk, K. G.; Ellerby, D. T.; Loehman, R. E. *J. Am. Ceram. Soc.* **1996**, *79*, 2497−2499.
(18) Duvauchelle, N.; Kesteman, E.; Oudet, F.; Bordes, E. *J. Solid State Chem.* **1998**, *137*, 311−324.
(19) Kumar, P.; Sandhage, K. H. *J. Mater. Sci.* **1999**, *34*, 5757−5769.
(20) Rogers, K. A.; Kumar, P.; Citak, R.; Sandhage, K. H. *J. Am. Ceram. Soc.* **1999**, *82*, 757−760.
(21) Wagner, F.; Garcia, D. E.; Krupp, A.; Claussen, N. *J. Eur. Ceram. Soc.* **1999**, *19*, 2449−2453.
(22) Schulmeyer, W. V.; Ortner, H. M. *Int. J. Refract. Met. Hard Mater.* **2002**, *20*, 261−269.
(23) Velev, O. D.; Jede, T. A.; Lobo, R. F.; Lenhoff, A. M. *Nature* **1997**, *389*, 447−448.
(24) Velev, O. D.; Jede, T. A.; Lobo, R. F.; Lenhoff, A. M. *Chem. Mater.* **1998**, *10*, 3597−3602.
(25) Holland, B. T.; Blanford, C. F.; Do, T.; Stein, A. *Chem. Mater.* **1999**, *11*, 795−805.
(26) Stein, A.; Schroden, R. C. *Curr. Opin. Solid State Mater. Sci.* **2001**, *5*, 553−564 and references therein.
(27) Dong. *Adv. Mater.* **2002**, *14*, 1506−1510.
(28) Barin, I. *Thermochemical Data of Pure Substances*; VCH: Weinheim, Germany, 1989.

tetraethyl orthosilicate (TEOS; 98%), titanium(IV) fluoride ($TiF_4$), and titanium(IV) propoxide were from Aldrich; hydrochloric acid (HCl; 37%) and nitric acid ($HNO_3$; 70%) were obtained from Mallinckrodt. All chemicals were used as-received without further purification. Water used in all syntheses was purified with a resistivity greater than 18 MΩ·cm. A type 316 stainless steel threaded pipe (10.2 cm long, 1.2 cm internal diameter) with two corresponding threaded 316 stainless steel caps was purchased from McMaster-Carr Supply Co. EpoxySet resin and hardener, silicon carbide abrasive paper, and aqueous/propylene glycol-based diamond suspensions were from Allied High Tech Products, Inc.

**Preparation of 3DOM $SiO_2$ and Spherical $SiO_2$ Preforms.** 3DOM $SiO_2$ preforms were prepared from colloidal crystal arrays of monodisperse PMMA spheres. PMMA spheres were prepared by a surfactant-free emulsion polymerization of MMA at 70 °C with 2,2′-azobis(2-methylpropionamidine) dihydrochloride initiator.[29] Centrifugation or gravity sedimentation of the resulting sphere suspension yielded colloidal crystalline arrays.[25] A 16.67 g sample of TEOS was mixed with 18.0 g of a 1 M $HNO_3$(aq) solution for 10−15 min to form a homogeneous sol. Stirring was stopped, and approximately 7 g of dried PMMA template was immersed in the precursor solution. After 1 min, the suspension was vacuum filtered until dry. The polymer−inorganic composites were aged for 1 day at room temperature, then heated at a rate of 2 °C $min^{-1}$ to 600 °C, and calcined in air at this temperature for 1 h to combust the polymer spheres and solidify the inorganic framework. The opalescent 3DOM $SiO_2$ preforms possessed smooth, nearly 60 nm thick walls and pore spacings of 334 or 367 nm (Figure 2, Table 1). Most regions of the preform had highly ordered structures with accessible porosity (Figure 2a), but other areas were partially obstructed by coatings of a thicker crust (Figure 2b,c). It is possible to avoid such coatings in careful preparations. However, in this investigation, they provided a means for comparing reactivities in silica regions having different extents of condensation. For comparison, silica spheres were prepared by the Stöber−Fink method.[30] They were used as preforms either as synthesized at room temperature or after annealing at 500 °C for 2 h.

**Preparation of a 3DOM $TiO_2$ Reference Sample.** A 3DOM $TiO_2$ sample (anatase) was prepared as a titanium reference sample for microprobe analysis, according to previous literature techniques.[31] The powder product was opalescent and purple in color as a result of its ordered macroporous structure.

**Pseudomorphic Conversion with $TiF_4$.** All reactants, the reaction pipe, and two titanium boats (1 cm wide, 3 cm long, 0.6 cm in height) were transferred into a nitrogen glovebox for assembly. The titanium boats were separately loaded with the 3DOM $SiO_2$ preforms and the modifying $TiF_4$ reactant material, using a Ti:Si ratio of 2:1 unless stated otherwise in the text. Typical amounts were 50 mg of the silica preform and 200 mg of $TiF_4$. The boats were inserted into the reaction pipe, which was sealed with threaded caps. The sealed pipe was removed from the glovebox, inserted into a quartz tube, and oriented in a tube furnace so that the 3DOM $SiO_2$ was at the upstream end of the tube furnace. Reaction vessels were then heated from ambient temperature to 190−300 °C at 5 °C $min^{-1}$ for 4 h in flowing Ar (0.5 L $min^{-1}$). Because the pipe experienced cooling from the flowing Ar, a slight thermal gradient existed between the $TiF_4$ (235 °C) and the silica preform (232 °C) with the oven temperature set at 250 °C. Any gaseous products (e.g., $SiF_4$(g)) could not be analyzed with the current experimental setup, but these would escape upon opening of the reactor tube. *$SiF_4$ is highly toxic and corrosive; therefore, the reaction pipe must be opened inside a fume hood, and protective clothing must be worn.*

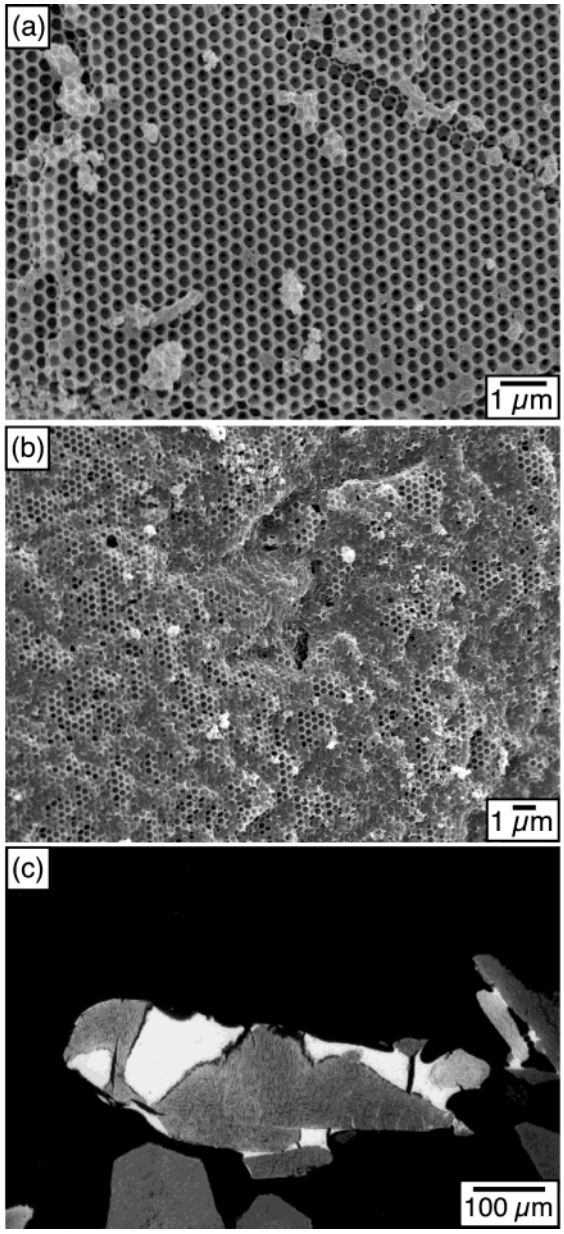


**Figure 2.** SEM images of a 3DOM $SiO_2$ preform used in these experiments: (a) 3DOM $SiO_2$ particle surface with highly accessible ordered porosity and smooth wall features; (b) 3DOM $SiO_2$ particle surface partially obstructed with a denser coating of $SiO_2$; (c) backscattered electron image of several 3DOM $SiO_2$ particles embedded in an epoxy resin. The lighter areas correspond to a denser surface similar to that shown in part b, and darker areas correspond to the open surfaces depicted in part a.

**Steam Treatment of $TiOF_2$ Samples.** Subsequent pseudomorphic transformation of macroporous $TiOF_2$ conversion products obtained at 235 °C was performed to yield macroporous $TiO_2$. The $TiOF_2$ samples were placed in ceramic crucibles and heated in flowing moist air inside a tube furnace at 300 °C for 4 h. The moist air was generated by passing air through room-temperature water.

**Characterization.** A JEOL 6500 field-emission gun scanning electron microscope was used to image the products at an accelerating voltage of 5 kV. Samples for electron microscopy were prepared by dusting a few milligrams of sample onto carbon conductive tabs supported by aluminum specimen mounts. Pt coatings of 10 nm were evaporatively applied to scanning electron microscopy (SEM) specimens that did not require electron probe compositional analysis. Energy-dispersive X-ray spectroscopy (EDS) and wavelength-dispersive

(29) Schroden, R. C.; Al-Daous, M.; Sokolov, S.; Melde, B. J.; Lytle, J. C.; Stein, A.; Carbajo, M. C.; Fernandez, J. T.; Rodriguez, E. E. *J. Mater. Chem.* **2002**, *12*, 3261−3327.

(30) Stöber, W.; Fink, A.; Bohn, E. *J. Colloid Interface Sci.* **1968**, *26*, 62−69.

(31) Schroden, R. C.; Al-Daous, M.; Blanford, C. F.; Stein, A. *Chem. Mater.* **2002**, *14*, 3305−3315.

**Table 1. Summary of Structural Feature Dimensions and Crystallite Sizes**

| sample | pore spacing[a] (nm) | wall thickness[a] (nm) | cube edge length[a] (nm) | crystallite size[b] (nm) |
|---|---|---|---|---|
| | Series 1 | | | |
| 3DOM $SiO_2$ preform | 367 ± 27 | 57 ± 21 | | |
| conversion with $TiF_4$, 235 °C | 366 ± 35 | | 96 ± 14 | 41 ± 5 |
| second conversion with steam, 300 °C | 356 ± 14 | | 123 ± 14 | 5 ± 1 |
| | Series 2 | | | |
| 3DOM $SiO_2$ preform | 334 ± 15 | 59 ± 12 | | |
| conversion with $TiF_4$, 235 °C (1)[c] | 342 ± 10 | | 83 ± 19 | 22 ± 1 |
| conversion with $TiF_4$, 235 °C (2)[c] | 339 ± 9 | | 133 ± 17 | 22 ± 1 |
| conversion with $TiF_4$, 235 °C (3)[c] | | | 121 ± 21 | 22 ± 1 |
| conversion with $TiF_4$, 300 °C | 281 ± 13 | | 133 ± 13 | 29 ± 1 |
| second conversion with steam, 300 °C | 322 ± 8 | | 132 ± 14 | 5 ± 1 |

[a] Dimensions obtained from SEM images. [b] Crystallite sizes calculated from XRD line broadening. [c] (1) refers to the region shown in Figure 7a, (2) to the region in Figure 3b, and (3) to the region in Figure 7b.

X-ray spectroscopy (WDS) microprobe measurements were performed at 15 kV with a JEOL 8900 electron probe microanalyzer to identify and quantify the elemental composition of selected samples. Samples for WDS microprobe analysis were mounted in epoxy resin, polished sequentially down to 1 $\mu$m grit sizes with SiC abrasive papers and monocrystalline diamond polishing suspensions, and coated with 10−15 nm of evaporated carbon. Spectra were processed, and elemental compositions were estimated by JEOL JXA-8900R version 3.02 software. 3DOM $SiO_2$ and 3DOM $TiO_2$ samples were used as standards for Si and Ti, because their solid volume filling fractions approximated those of pseudomorphic products more closely than denser oxide standards would. A geological sample of fluorapatite ($Ca_5(PO_4)_3F$) was chosen as a standard for F, and the experimentally determined composition of the standard was used for calculations of F content. This sample was not porous, making it necessary to adjust the raw F weight percent data obtained from 3DOM conversion products by their estimated solid volume filling fractions (ca. 30%). The $TiOF_2$ content was calculated from the F weight percent data and the $TiO_2$ content from the difference between the total Ti weight percent and the weight percent of Ti assigned to $TiOF_2$. Therefore, uncertainties of ±5% in the solid volume filling fraction could introduce errors of up to 7 wt % for the $TiOF_2$ and $TiO_2$ contents. The silica content was not affected by these estimates, since it was determined without the fluorapatite standard. The WDS measurement protocol was to identify regions of low density/high porosity with backscattered electron imaging and measure 20 points in these areas per sample. Powder X-ray diffraction (XRD) patterns were collected on a Bruker AXS microdiffractometer with Cu Kα radiation generated at 45 kV and 40 mA. Unaligned single-crystal quartz slides served as substrates for these measurements. XRD patterns were processed using Jade software, and crystallite sizes were estimated from line broadening and the Scherrer equation. BET specific surface areas were calculated from nitrogen adsorption data measured on an Advanced Scientific Designs RXM-100 catalyst characterization instrument. At least five data points were used per adsorption measurement, each of which was carried out in triplicate.

## Results and Discussion

Under optimized conditions, pseudomorphic transformations of large sample regions were observed on various length scales in conversion reactions from silica to titanium oxyfluoride and subsequently to titanium dioxide. In this discussion, we will first describe the observed structural and compositional changes under favorable conditions, and then discuss effects of modifying the synthesis conditions and kinetic effects on the transformations. Two independent preform series were studied (Table 1). Both series behaved similarly. For convenience, the data below correspond to samples for series 2 in Table 1, unless otherwise stated.

**Transformation of 3DOM $SiO_2$ to 3DOM $TiOF_2$ at 235 °C.** The products obtained at 235 °C were light gray in color and exhibited strong green and pink opalescence (optical (111) stop band at 604 nm, compared to 578 nm for the 3DOM $SiO_2$ preform), giving a visual confirmation of the success of the pseudomorphic transformation on an extended length scale. The red-shifted opalescent color was consistent with an increased refractive index and/or greater thickness of the 3DOM walls for materials with similar pore spacings.[31] The mixture of opalescent colors may be due to angular dependence of reflected light from the ordered macroporous framework and a heterogeneous product composition that resulted in multiple indices of refraction. The BET specific surface area of the sample (26 $m^2\ g^{-1}$) was greatly reduced from the surface area of the preform (213 $m^2\ g^{-1}$). SEM imaging of this product revealed 3DOM domains covering tens of micrometers with pore spacings nearly identical to those of the 3DOM $SiO_2$ preform (Figure 3a, Table 1). Approximately half of the converted sample displayed this degree of order. The smooth wall structure of the preform had been transformed into fused cubes with edge lengths of 133 ± 17 nm (Figure 3b). XRD partially confirmed the chemical conversion of the sample and indicated that the cubes were polycrystalline $TiOF_2$ with average grain sizes of 22 ± 1 nm (Figure 4b). No reflections corresponding to crystalline $TiO_2$ were observed, although amorphous $TiO_2$ may have been present. O, F, Si, and Ti were detected by EDS, with the notable absence of Fe from the reaction pipe. Compositional estimates of the sample's ordered regions by WDS microprobe analysis indicated that ca. 2/3 of the sample had been converted to $TiOF_2$, 1/3 was unreacted silica, and possibly ca. 3% of the material consisted of amorphous titania (Table 2).

**Transformation of 3DOM $TiOF_2$ to 3DOM $TiO_2$ in Steam at 300 °C.** A subsequent reaction was then pursued which resulted in dual pseudomorphic conversions of both the converted 3DOM structure and the cubic crystallites. The macroporous $TiOF_2$ product was treated with moist air at 300 °C for 4 h to attempt the following reaction:[32]

$$TiOF_2(s) + H_2O(g) \rightarrow TiO_2(s) + 2HF(g) \qquad (3)$$

SEM analysis of the product revealed preservation of

(32) Machin, J. S.; Deadmore, D. L. *Nature* **1961**, *189*, 223−224.

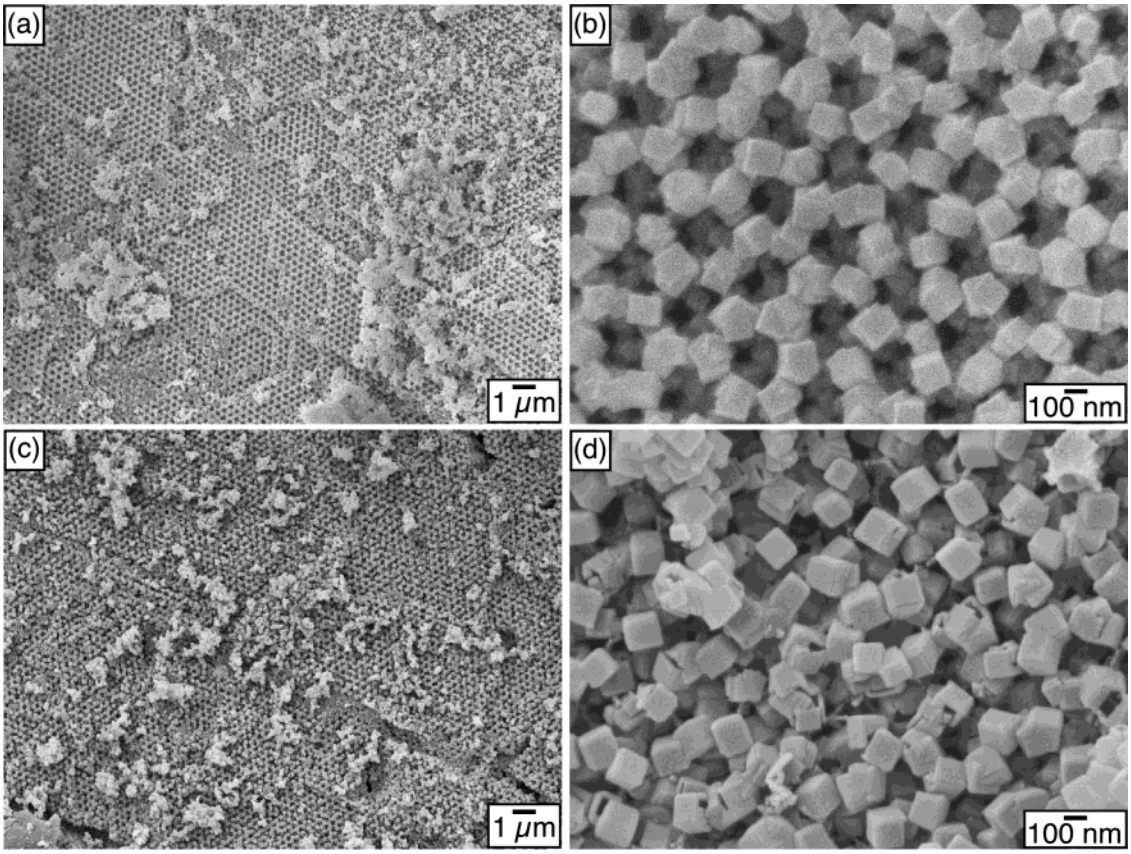


**Figure 3.** SEM images of $TiOF_2$ and $TiO_2$ conversion products. (a) 3DOM $TiOF_2$ obtained by heating 3DOM $SiO_2$ with $TiF_4$ at 235 °C, 4 h, exhibits pseudomorphism over tens of micrometers. (b) A higher resolution image shows that the skeleton of 3DOM $TiOF_2$ is composed of interconnected $TiOF_2$ cubes. (c) 3DOM $TiO_2$ obtained by steaming 3DOM $TiOF_2$ at 300 °C, 4 h, displays structural retention over tens of micrometers. (d) This image obtained at higher magnification shows that the cubic shapes of particles forming the framework were also preserved in the transformation to titania. Some cubes appeared to be hollow.

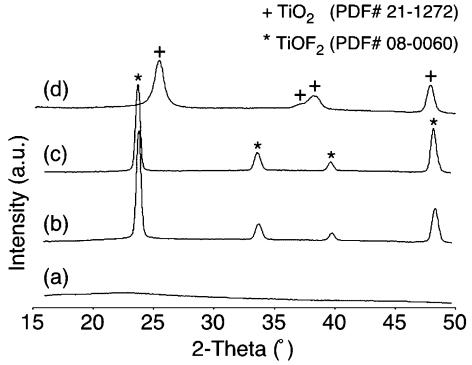


**Figure 4.** Micro X-ray diffraction patterns of (a) the 3DOM $SiO_2$ preform, (b) the conversion product obtained from 3DOM $SiO_2/TiF_4$ at 235 °C, (c) the conversion product obtained from 3DOM $SiO_2/TiF_4$ at 300 °C, and (d) the final product obtained after treatment of the $TiOF_2$ product from (b) with water vapor at 300 °C for 4 h.

both the macropores (with a slightly reduced pore spacing of 322 ± 8 nm) and wall skeleton morphologies (cube edge length 132 ± 14 nm) over length scales of tens of micrometers (Figure 3c). Interestingly, some nanocubes appeared open and hollow, suggesting that $TiO_2$ may have formed at cube surfaces from internal $TiOF_2$ reactant (Figure 3d). XRD showed only anatase $TiO_2$ reflections (PDF No. 21-1272) with greatly reduced grain sizes of 5 ± 1 nm (Figure 4d), indicating the polycrystalline nature of individual cubes. Compositional estimates by WDS analysis revealed that most $TiOF_2$ had been converted to $TiO_2$, and that the silica content of the sample was significantly lower compared to that of the preform (Table 2), probably by reaction with HF byproduct according to

$$SiO_2(s) + 4HF(g) \rightarrow SiF_4(g) + 2H_2O(g) \qquad (4)$$

In this way, we have demonstrated a two-step pseudomorphic conversion sequence with the interesting ability to reproduce cubes of cubic $TiOF_2$ into tetragonal anatase $TiO_2$ with the same morphology and to replicate the three-dimensionally ordered macroporosity of the initial silica preform. The resulting 3DOM $TiO_2$ has a different wall texture than 3DOM $TiO_2$ prepared directly by colloidal crystal templating of titanium alkoxide precursors.[33,34] In the latter materials, smoother, more continuous wall surfaces were formed in the presence of spherical polymer templates, whereas in the pseudomorphic transformation, the cubic $TiOF_2$ preform dictated the titania morphology, resulting in a more angular surface.

**Parameters Influencing the Conversion of Silica to $TiOF_2$.** Each of the conversion steps is controlled by both thermodynamic and kinetic parameters. We investigated these by studying the effects of temperature, relative amounts of reactants, and preform structural

(33) Holland, B. T.; Blanford, C. F.; Stein, A. *Science* **1998**, *281*, 538−540.
(34) Stein, A. *Microporous Mesoporous Mater.* **2001**, *44*−*45*, 227−239.

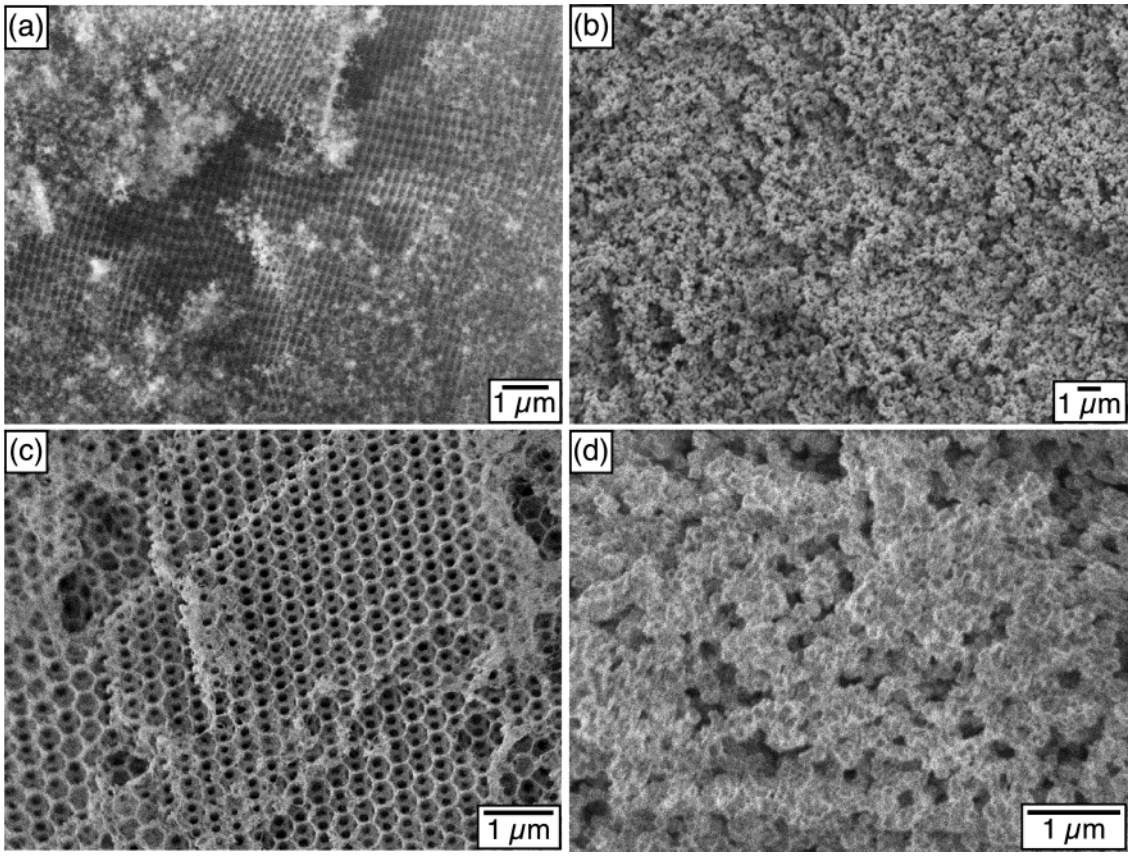


**Figure 5.** SEM images of conversion products obtained by regulating the temperature and the Ti:Si reagent ratio in the reaction with $TiF_4$ and 3DOM $SiO_2$. (a) No cubic nanocrystals were formed at 190 °C (2 Ti:1 Si). (b) At 300 °C (2 Ti:1 Si) the ordered geometry was lost. (c) No visible changes to the 3DOM preform were observed at 1 Ti:1 Si (235 °C). (d) Intense crystallite growth dominated the structure at 5 Ti:1 Si (235 °C). (Figure 5a corresponds to data series 1, and all other images correspond to data series 2 in Table 1.)

**Table 2. Quantitative Electron Microprobe Analysis of Conversion Product Compositions**

| sample | est filling fraction (%) | [$SiO_2$] (wt %) | [$TiO_2$] (wt %) | [$TiOF_2$] (wt %) |
|---|---|---|---|---|
| conversion with $TiF_4$, 235 °C | 30 | 30 | 3 | 67 |
| conversion with $TiF_4$, 300 °C | 50 | 6 | 37 | 57 |
| second conversion with steam, 300 °C | 30 | 8 | 87 | 5 |

features on product compositions and morphologies. Heterogeneities in the products provided further information about the reaction progress and mechanism.

*Effects of Reaction Temperature.* Various reaction temperatures were selected to examine the influence of temperature on the chemical composition and the degree of structural retention of the transformed product. Initial reactions were attempted at 900 °C, as suggested by a past report of thermodynamic feasibility for this reaction,[5] but at this high temperature, no solid product remained in the reaction boat containing the preform. Substantially milder processing conditions were then investigated to decrease preform reactivity. Reactions at 190, 235, and 300 °C were aimed at utilizing the relatively high vapor pressure of $TiF_4$ (<2, ~100, and ~760 Torr, respectively) for chemical conversion and shape preservation on a nanoscale. At 190 °C, virtually no conversion occurred. The product was morphologically identical to the 3DOM $SiO_2$ preform according to SEM images (Figure 5a), having smooth walls and color and opalescence similar to those of the starting material. No reflections from crystalline material were observed in the XRD pattern, which showed only the broad diffraction features also found in the amorphous 3DOM silica preform (Figure 4a). EDS detected only O and Si. At 235 °C, the ordered product discussed earlier could be formed. At 300 °C, i.e., above the sublimation temperature of $TiF_4$, an irregular product consisting of small cubic crystallites with edge lengths of 133 ± 13 nm was observed by SEM (Figure 5b, Table 1). The product had visually changed from the white color and bright green opalescence of the 3DOM $SiO_2$ preform to a light gray with some strongly attenuated pink opalescence. The reduction in opalescence was due to the significant decrease in the product's ordered macroporosity, although ordered morphologies were partially retained. XRD analysis indicated the presence of cubic $TiOF_2$ with a crystallite size of 29 ± 1 nm (Figure 4c). No other crystalline phases were detected, and almost no amorphous background was visible, although WDS analysis suggested that more amorphous titania may have been present than in the material prepared at 235 °C (Table 2). The silica content of this sample was significantly less than in the lower temperature product. These studies indicated that the temperature window for successful pseudomorphic transformations of nanostructured silica to $TiOF_2$ is relatively narrow.

*Effects of Reagent Ratios.* Product structures and compositions were also sensitive to precursor ratios and reaction atmosphere. Controlling the molar ratio of Ti to Si allowed regulation of the extent of pseudomorphic conversion. Experiments performed with molar ratios of 1:1, 2:1, and 5:1 $TiF_4$:3DOM $SiO_2$ at 235 °C for 4 h showed no reaction (Figure 5c), partial pseudomorphic conversion (Figure 3b), and strong conversion without pseudomorphism (Figure 5d), respectively. The increased extent of transformation was due to increasingly larger excesses of reactants that drove the reaction (eq 2) further toward completion. It was important that the reaction pipe was sealed to allow the accumulation of $TiF_4$(g) for significant conversion. In addition, poorly sealing vessels may promote excessive convection that could disturb the nucleation and growth of modifying species. The use of fresh $TiF_4$ was also essential since the salt readily hydrolyzes with atmospheric moisture. Reactor assembly in an inert atmosphere was therefore critical for reproducing results.

*Effects of Preform Structure.* Pseudormorphic conversion reactions were studied using preforms with various shapes and feature sizes to better understand transformations over a range of length scales. Several size regimes were addressed with 3DOM $SiO_2$ preforms. Shape preservation with sub-100 nm resolution was observed in the formation of anatase $TiO_2$ nanocubes using water vapor. This process cleanly replicated the exterior of cubic particles with anatase nanocrystallites, and could be applicable to the pseudomorphic conversion of other fluoride-bearing preforms. At a slightly larger scale, 3DOM $SiO_2$ was reproduced with ca. 100 nm resolution via $TiOF_2$ nanocubes. At the largest scale of pseudomorphism, ordered domains of tens of micrometers were observed by SEM and by the opalescence of the product. Aggregated silica sphere preforms (diameter 587 ± 28 nm, BET surface area 7.3 $m^2\ g^{-1}$) were also examined to see the effects of shape, dimensions, and degree of condensation on the conversion reaction (Figure 6). When unannealed silica spheres were used, no solid material remained in the precursor boat under conditions that were successful for calcined 3DOM $SiO_2$ preforms. The as-prepared materials had a low degree of condensation with a high content of reactive ≡Si—OH groups that were readily attacked by fluoride ions. Although gaseous products could not be studied with the equipment used, it is possible that such vapors (e.g., $SiF_4$) carried material away from the preform. Annealed preforms yielded spheroidal particles (diameter 754 ± 98 nm) with a rough surface composed of fused cubic nanocrystallites. Sintering between cubic grains bridged several spheroidal particles, creating small agglomerations. The greater thickness and lack of mesoporosity of the annealed silica spheres, compared to the walls of 3DOM $SiO_2$, resulted in a different product structure. Rather than being transformed throughout, many spheres were either fully or partially coated with a surface layer of $TiOF_2$ crystals on top of the smooth silica substrate. In contrast, 3DOM walls were sufficiently thin to permit the complete conversion of framework features. For these reasons, limited pseudomorphism on a submicrometer scale was achieved with $SiO_2$ sphere preforms. During submission of this paper, the pseudomorphic solid—gas transformation of another type of silica preform, diatomic silica, to $TiOF_2$ and $TiO_2$ was reported.[35]

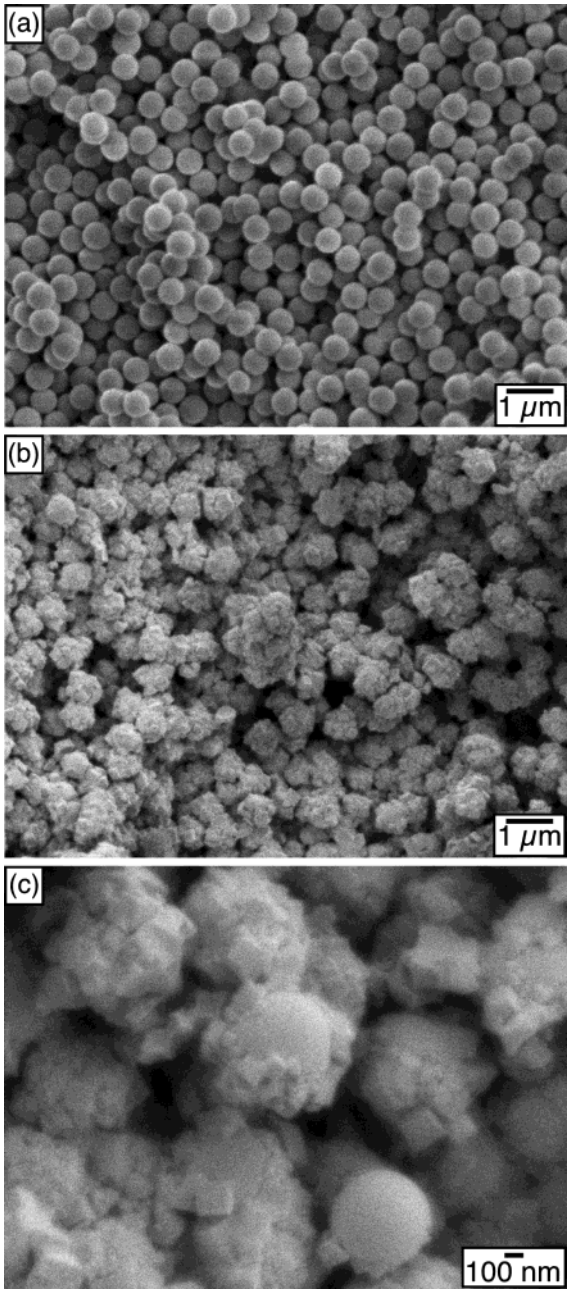


**Figure 6.** SEM images of (a) a $SiO_2$ sphere preform used to investigate pseudomorphism on a larger scale and (b) the conversion product obtained at 235 °C showing coarse reproduction of spherical geometry. (c) In some particles, a coating of fused nanocrystallites formed at the sphere surface.

**Discussion of the $SiO_2$ to $TiOF_2$ Transformation Mechanism.** In pseudomorphic conversion processes, such as these, reactions can occur at intergranular boundaries (reaction-controlled), in the silica-rich phase (diffusion-controlled), or in the product-rich phase (diffusion-controlled).[22] Two main mechanistic models have been described for bulk conversions. In the shrinking core model a product layer grows on the surface of the preform during its reaction with the gaseous precursor and grows inward, causing the core to shrink until the

(35) Unocic, R. R.; Zalar, F. M.; Sarosi, P. M.; Cai, Y.; Sandhage, K. H. *Chem. Commun.* **2004**, 796—797.

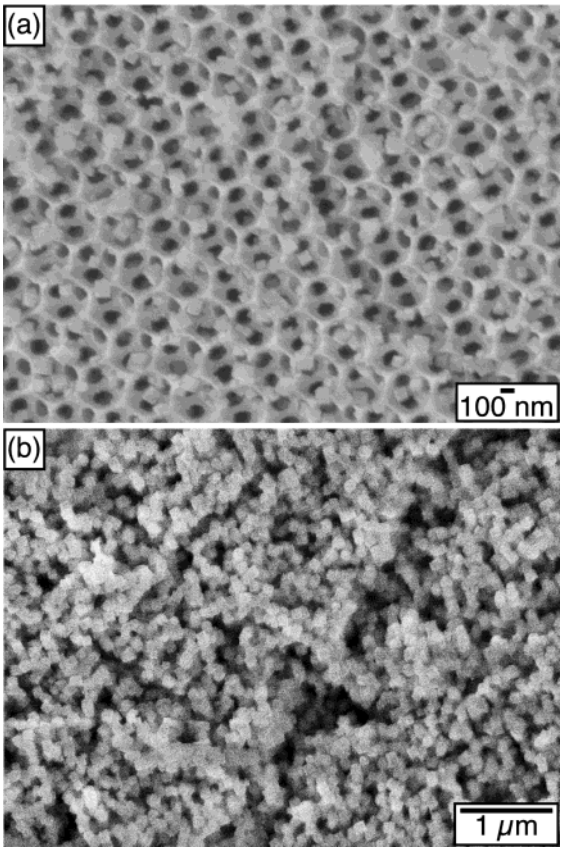


**Figure 7.** SEM images of selected sample regions provide information about the kinetic stages of the conversion reaction carried out at 235 °C for 4 h: (a) initial nucleation of cubic crystallites on 3DOM nanostructured surfaces; (b) loss of ordered structure via excessive crystallite formation. Compare with Figure 3a,b, an ordered region in the same sample.

preform is completely converted to product.[22,36] In the crackling core model, an initially nonporous preform particle incurs cracks from the surface to the center as it reacts with a gas. The newly introduced pores facilitate further reaction with the gas.[22,37] When the preforms are already porous, as in 3DOM $SiO_2$, crack formation is not necessary to allow efficient gas penetration into the preform. Even though a complete understanding of the pseudomorphic transformation mechanisms of the nano/microstructured materials considered here will require more detailed studies, some mechanistic information about the reactions is available from the current data.

Formation of $TiOF_2$ from $TiF_4$ requires an oxygen source, which is provided by the silica preform. In the case of unannealed silica spheres, some oxygen may also have been furnished by surface-adsorbed water, resulting in formation of HF and $SiF_4$, and the observed loss of solid material. Surface-adsorbed water was much less likely a factor in the calcined materials, and the large reduction in surface area from 213 $m^2\ g^{-1}$ for the 3DOM $SiO_2$ preform (due to structural mesoporosity)[25] to 26 $m^2\ g^{-1}$ for the $TiOF_2$ conversion product (due to the external surface of the $TiOF_2$ particles, combined with some textural mesoporosity) attests to the consumption

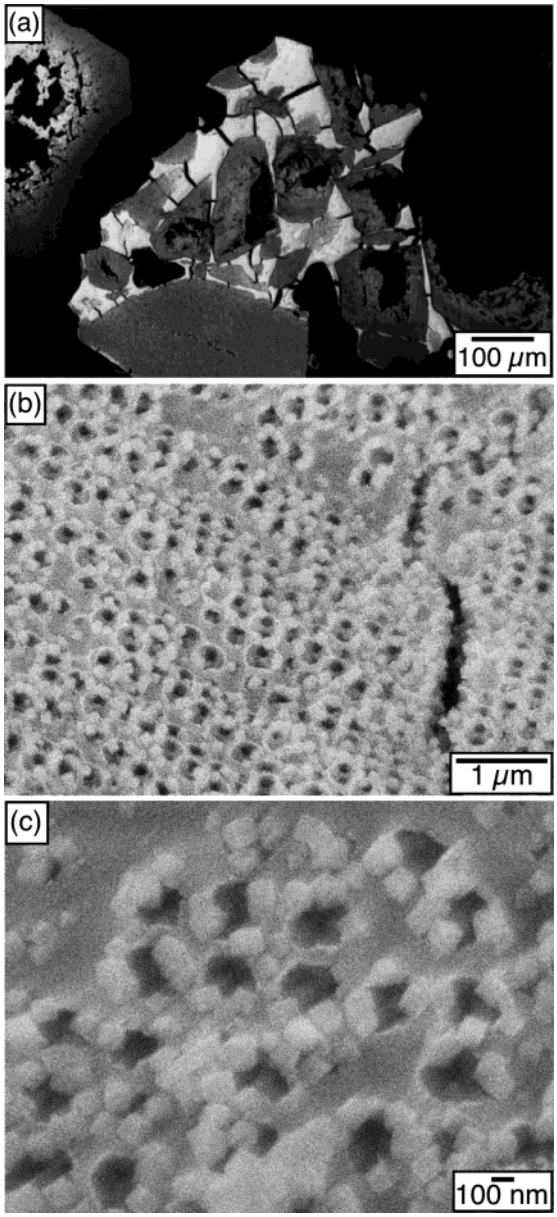


**Figure 8.** SEM images of the conversion product formed by treating nonuniform 3DOM silica with $TiF_4$ at 235 °C for 4 h. (a) Backscattered electron image of an epoxy-embedded, converted particle (235 °C treatment with $TiF_4$ for 4 h). Microprobe analysis indicated that the denser, lighter regions consisted mostly of unconverted silica, while conversion to $TiOF_2$ predominated in the more accessible, darker regions. (b) Growth of cubic nanocrystallites along macropore rims and crack edges. (c) Crystallite nucleation was limited to pore openings and not observed on some denser $SiO_2$ coatings.

of mesoporous silica in this sample. If significant amounts of mesoporous silica had still been present, a higher final surface area would have been expected.

The stages of $TiOF_2$ growth could be observed in the 3DOM $SiO_2$ sample reacted with $TiF_4$ at 235 °C, which displayed some heterogeneity due to kinetic effects. The SEM images in Figures 7a, 3b, and 7b show progressively larger degrees of conversion. Cubic $TiOF_2$ nanocrystals initially nucleated on the surface of the preform, often in the thinner strut regions, but also at intersections of struts (Figure 7a). As growth continued, the silica framework was displaced by continuous arrays of cubes, whose orientation appeared to be dictated by the

(36) Yagi, S.; Kunii, D. *Fifth Symposium on Combustion*; Combustion Institute: Pittsburgh, PA, 1955; pp 231−244.
(37) Park, J. Y.; Levenspiel, O. *Chem. Eng. Sci.* **1975**, *30*, 1207−1214.

skeleton of the preform, as crystals were interconnected only weakly at cube corners (Figure 3b). These observations point toward a shrinking core model, which led to clean reproduction of the 3DOM structure by $TiOF_2$ cubes over domain sizes of tens of micrometers. SEM images confirmed continued interconnectivity of the voids, ensuring accessibility to relatively large internal surface areas. Upon further reaction (Figure 7b), at higher temperatures (Figure 5b), or with a greater excess of $TiF_4$ (Figure 5d), cubes agglomerated, resulting in a more disordered structure, albeit a low density was maintained.

Regions of the 3DOM silica preform that were coated with a denser silica layer provided some information about the location of reactive sites. Figure 8a shows a backscattered electron image of particles that had been exposed to $TiF_4$ at 235 °C for 4 h. As in the corresponding image of the preform (Figure 2c), lighter areas correspond to greater densities in the material. Local microprobe analysis by WDS indicated that the denser areas still consisted mostly of unconverted $SiO_2$, while the more accessible, porous regions were mostly converted to $TiOF_2$. The SEM images of partially encrusted regions (Figure 8b,c) reveal growth of cubic crystallites primarily at macropore rims and along cracks in the particles but virtually no growth on the smoother, densified surfaces. Crystal growth could be favored at these sites by enhanced reactivity from elevated energetics and strain and a greater presence of surface hydroxyl groups and exposed Si−O−Si sites.

In the case of the spherical preforms, the shrinking core model also seems to be suitable to describe the transformation. The greatly increased sphere diameter of the product and the nanocrystal skin on top of a smooth curved sublayer observed for some particles suggest that initial growth occurred at the sphere surfaces. Penetration of $TiF_4$ to the core was less facile in the thicker, nonporous, spherical particles, compared to the thin, mesoporous 3DOM walls. In this case, chemical vapor transport (CVT) processes may have competed with the pseudomorphic transformation,[22] where intermediate gaseous transport phases produced from one sphere could deposit on another sphere, creating a growth layer. Again, a different experimental setup will be required to monitor gas phases and verify this hypothesis. In addition to solid−gas displacement reactions, sintering occurred, resulting in agglomeration of multiple spheres.

## Conclusions

This study has demonstrated the feasibility of a multistep pseudomorphic conversion of amorphous $SiO_2$ to crystalline $TiO_2$ with a resolution of approximately 100 nm, but has also highlighted the importance of kinetic control in addition to thermodynamic criteria. For nanostructures, pseudomorphism may only be obtained within a limited temperature window. The comparison of silica preforms showed that factors such as preform dimensions, porosity, and degree of condensation strongly influence the extent of transformation. It is anticipated that variations in preform treatment, reaction times, temperatures, and ratios of reactants can permit further fine-tuning of the balance between structure retention and the maximum degree of chemical conversion. Pseudomorphic transformations have the potential of becoming powerful new methods for structuring micro- and nanomaterials with complex 3D architectures that may be readily formed in one composition (e.g., silica) but more difficult to form in another composition. The synthetic paradigms demonstrated for the silica to anatase conversion may be transferable to other 2D or 3D material shapes within the applicable range of feature sizes. Future conversions of additional interesting 3DOM compositions, lithographically patterned devices, and other nanoarchitectured solids are also envisioned.

**Acknowledgment.** This research was funded in part by the MRSEC program of the NSF (Grant No. DMR-0212302), the Office of Naval Research (Grant No. N00014-01-1-0810, subcontracted from NWU), and the U.S. Army Research Laboratory and the U.S. Army Research Office (Grant DAAD 19-01-1-0512). We thank the Electron Microprobe Laboratory in the Department of Geology and Geophysics at the University of Minnesota for compositional analysis. R.T.T. gratefully acknowledges a fellowship through the University of Minnesota Lando/NSF-REU summer program.

CM049489B